AMERICAN ACADEMY OF OPHTHALMOLOGY®

Alterations in the Choroidal Sublayers in Relationship to Severity and Progression of Diabetic Retinopathy

A Swept-Source OCT Study

Erica W.T. Kung, MBChB, Victor T.T. Chan, MBChB, Ziqi Tang, MPhil, Dawei Yang, MBBS, Zihan Sun, MBBS, Yu Meng Wang, PhD, C.H. Chan, Michael C.H. Kwan, Jian Shi, MSc, Carol Y. Cheung, PhD

Purpose: To examine the association of baseline choroidal sublayers metrics with the risk of diabetic retinopathy (DR) progression over 2 years, with adjustment for confounding factors that affect choroidal measurements.

Design: Prospective, observational cohort study.

Participants: One hundred three eyes from 62 patients with diabetes mellitus (DM).

Methods: Patients were followed up at 6-month intervals for at least 2 years. Choroidal metrics including choroidal area, choroidal thickness (CT), and choroidal vascularity index were measured for both (1) the choriocapillaris plus Sattler's layer and (2) the Haller's layer within the subfoveal and parafoveal region. Cox proportional models were constructed to estimate the relationship between baseline choroidal metrics and DR progression, adjusted for intereye correlation, established risk factors (i.e., duration of DM, glycated hemoglobin [HbA_{1c}] level, body mass index [BMI], use of insulin, and mean arterial blood pressure [MABP]) and confounding factors of choroidal measurements (i.e., age and axial length). Additional predictive value of choroidal metrics was assessed using the C-statistic.

Main Outcome Measures: Hazard ratios (HRs) calculated by Cox proportional hazards model to demonstrate the associations between baseline choroidal metrics and DR progression.

Results: After adjusting for age, axial length, and intereye correlation, choroidal metrics in Haller's layer at baseline that were associated with a higher risk of DR progression included increases in subfoveal choroidal area (HR, 2.033; 95% confidence interval [CI], 1.179–3.505; $P = 0.011$), subfoveal plus parafoveal choroidal area (HR, 1.909; 95% CI, 1.096–3.326; $P = 0.022$), subfoveal CT (HR, 2.032; 95% CI, 1.181–3.498; $P = 0.010$), and subfoveal plus parafoveal CT (HR, 1.908; 95% CI, 1.097–3.319; $P = 0.022$). These associations remained statistically significant after additionally adjusting for duration of DM, HbA_{1c} level, BMI, use of insulin, and MABP. Addition of these choroidal metrics significantly improved the discrimination for DR progression when compared with established risk factors alone (e.g., duration of DM and HbA_{1c}; increase in C-statistic ranged from 8.08% to 9.67% [$P < 0.05$]).

Conclusions: Eyes with a larger choroidal area and CT in Haller's layer at baseline were associated with a higher risk of DR progression over 2 years. *Ophthalmology Science 2022;2:100130* © *2022 by the American Academy of Ophthalmology. This is an open access article under the CC BY-NC-ND license (http://creativecommons.org/licenses/by-nc-nd/4.0/).*

Supplemental material available at www.ophthalmologyscience.org.

Diabetic retinopathy (DR) is the leading cause of preventable blindness[1] and is the most common microvascular complication of diabetes mellitus (DM).[2] The pathogenesis of DR has been attributed primarily to the dysregulation of the retinal vasculature and subsequent destruction of the blood–retinal barrier.[3,4] However, recent evidence also suggests an additional role of the choroid,[5–9] which provides the major blood supply to the outer layers of the retina and the avascular fovea, responsible for nourishing the highly metabolically active photoreceptor cells as well as removing metabolic waste from the retinal pigmented epithelium.[10] Previous histopathologic studies have already revealed choroidal changes in diabetes, including microaneurysms, choriocapillaris loss, drusenoid deposits on Bruch's membrane, and choroidal neovascularization.[11–13] These findings were further confirmed using indocyanine green angiography, which showed reduced blood flow and vascular compromise in the subfoveal choroid.[14]

https://doi.org/10.1016/j.xops.2022.100130
ISSN 2666-9145/22

Given the important role of choroidopathy in diabetic eyes, different studies have evaluated the choroidal changes in patients with DR *in vivo* using spectral-domain OCT and enhanced depth imaging OCT. When compared with patients without DM, patients with DM but without DR showed significant reductions in choroidal vascularity index (CVI),[15] choroidal thickness (CT),[16–18] and choroidal blood flow[9] (refer to a recent meta-analysis by Endo et al[19]). However, regarding choroidal changes in different stages of DR, most of the previous studies are of cross-sectional design and yielded heterogeneous results, as shown in Table S1.[5,15–18,20–46] Although some studies reported an increase in CT with DR severity, other studies reported a decrease in CT or a lack of significant correlation between CT and DR. One of the potential sources of the discrepancy is that most of the previous studies did not adjust for the confounding factors that affect CT. Recent studies have shown that CT reduces with older age and elongated axial length[47–49] in healthy eyes. In DM, several studies also found that choroidal thinning is associated with higher glycated hemoglobin (HbA_{1c}) level,[22,50] longer duration of DM,[31] and previous treatment by panretinal photocoagulation.[34] These observations indicate the importance of the adjustment when researchers compile data on CT. Also, the role of choroidal metrics in predicting the progression of DR remains unknown.

In addition, changes in choroidal sublayers in diabetic eyes remain unclear. Anatomically, the choroidal vasculature comprises small vessels in the superficial choriocapillaris, medium vessels in Sattler's layer consisting of mostly choroidal arterioles, and large vessels in the deepest Haller's layer composed of mostly choroidal veins.[51] Given the role of choroidopathy in DR and the extensive damage of DM to the vasculature, more detailed evaluation of the choroidal sublayer changes in diabetic eyes is warranted. However, this knowledge gap was not addressed by most of the previous studies, because enhanced depth imaging spectral-domain OCT used in these studies has limited ability in visualizing the choroid–sclera interface (CSI) and the choroidal sublayers, particularly in Asian eyes.[52,53] The development of state-of-the-art swept-source (SS) OCT provides much better visualization of the choroid, especially the CSI and the choroidal sublayers (i.e., choriocapillaris plus Sattler's layer and Haller's layer).[52] This can be attributed to the different light source (wavelength-tunable laser) and longer laser wavelengths (1040–1060 nm) in SS OCT, which enhances penetration into the choroid and reduces scattering and dispersion from the retinal pigment epithelium and the choroid.[54,55] Swept-source OCT also results in higher reliability and repeatability in the measurement of CT.[56–58]

Therefore, this study aimed to evaluate the association between the choroidal sublayers metrics at baseline using SS OCT and the risk of DR progression, with adjustment for the confounding factors that affect choroidal measurements. We hypothesized that choroidal sublayers measured with SS OCT are associated with the risk of DR progression.

Methods

Participants

This was a prospective, observational cohort study with participants recruited consecutively from the Chinese University of Hong Kong Eye Centre, Hong Kong Eye Hospital, from July 2015 through January 2019. The study design adhered to the tenets of the Declaration of Helsinki and was approved by the research ethics committee of Hong Kong Eye Hospital. Written informed consent was obtained from all participants or their respective primary caregivers after a detailed explanation of the study.

Patients were eligible for the study if they fulfilled all of the following inclusion criteria: (1) age $\geq$ 18 years, (2) having a diagnosis of type 1 or 2 DM as defined by the American Diabetes Association, (3) spherical refractive error within the range of −8.5 to +4.0 diopters with $<$ 5.0 diopters of the cylinder, and (4) visual acuity (VA) not worse than Snellen 20/200. Exclusion criteria for study eyes included: (1) proliferative DR (PDR) at baseline; (2) eyes with prior retinal surgery, intravitreal injection, macular laser photocoagulation, or panretinal laser photocoagulation; (3) eyes with pathologic features that interfere with imaging (e.g., dense cataract or corneal ulcer); (4) eyes with ungradable SS OCT images; (5) diabetic macular edema (DME); and (6) glaucoma. We excluded participants with DME because previous studies have shown that CT was associated with DME.[15,16,18,21,22]

All participants were followed up consecutively for at least 2 years. All participants attended the second visit 6 months after the baseline examination. Whereas participants without DR and those with only mild nonproliferative DR (NPDR) were followed up annually afterward, those with moderate or severe NPDR were followed up every 6 months. In each visit, all participants underwent comprehensive ophthalmic and general medical examinations, including mean arterial blood pressure (MABP), weight, and height measurement; measurement of Snellen VA, intraocular pressure, autorefraction, axial length, and central corneal thickness; slit-lamp biomicroscopy; and dilated fundus examination. The MABP was measured according to the local guideline using a digital automatic blood pressure monitor (Avant 2120; Nonin Medical, Inc). Visual acuity was assessed for both eyes using a Snellen chart at a distance of 6 m, with the nontested eye covered. The best VA for each eye was recorded using metric notation from the Snellen chart and converted into the logarithm of the minimum angle of resolution units. Optical biometry was used to assess the axial length, and a mean value was calculated based on 5 measurements.

We also reviewed the latest medical record of the study participants to assess DM-associated factors, including the duration of DM, results of fasting lipid profile, and HbA_{1c} level. History of associated systemic diseases and other DM complications were elicited from interview-based questionnaires, and the information was checked further and confirmed from each patient's medical records by physicians.

Choroidal OCT Image Acquisition

After pupil dilatation, all study eyes underwent OCT examination with a commercially available SS OCT (Triton DRI-OCT; Topcon), which has a central wavelength of 1050 nm, a scanning speed of 100 000 A-scans/second, and a depth resolution of 8 μm. The choroid was imaged using the radial scanning protocol, which captures a 12 × 9-mm cross-sectional scan centered at the fovea.

Image quality control was performed independently by 2 readers (E.W.T.K. and V.T.T.C.) in the Chinese University of Hong Kong Ocular Reading Centre. The readers were masked to all patient characteristics, including DR severity and other retinal

pathologic features. OCT images with significant image artifacts and poor image quality were excluded from subsequent analysis, including (1) a quality score of < 80, (2) motion artifacts, (3) signal loss, and (4) noncentration (i.e., the fovea was not at the center of the image). When both graders determined that the boundaries of the choroidal sublayers were clearly distinguishable, the image was deemed gradable and used for the subsequent analyses.

Measurement of Choroidal Vascular Parameters

Eligible raw SS OCT images were loaded on a public domain software, Image J version 1.53 (National Institutes of Health, Bethesda, MD). Investigators who conducted the choroidal measurements were masked to all participants' clinical information. The horizontal B-scan image passing through the fovea horizontally was chosen for each eye. Using the segmented lines tool in ImageJ, 3 structures were delineated manually and outlined on each image, including the retinal pigment epithelium−Bruch's membrane interface, the lower border of Sattlers' layer, and the CSI (Fig 1). By this method, the choroid was segmented into 2 layers. The inner choroidal layer includes the region between the Bruch's membrane and the lower border of Sattler's layer and corresponds to the choriocapillaris and Sattler's layer (small to medium choroidal vessels). The choriocapillaris layer and the Sattler's layer were analyzed together as a complex because the choriocapillaris layer forms only 5% to 10% of the choroid[59] and delineation of this layer individually is difficult. The outer choroidal layer includes the region between the lower border of the Sattler's layer and the CSI, which corresponds to Haller's layer (large choroidal vessels). The border between Sattler's and Haller's layer was demarcated based on the morphologic features (mainly difference in choroidal vessel diameter between 2 layers). The mean diameter of the smallest large choroidal vessels in the Haller's layer was reported to be 100 μm and has been used as a cutoff for defining Haller's layer in choroidal vasculature analysis.[60]

Eligible raw SS OCT images were also processed using the protocol as previously described with modifications (Fig 2).[53,61–64] Briefly, the images were converted to 8-bit images and binarized by modified Niblack auto local thresholding, which gave the mean pixel value with standard deviation for all points. Whereas the dark pixels represented the luminal or vascular area, the light pixels corresponded to the stromal or interstitial component of the choroid. The annotated OCT images were then loaded on a custom-written application in Python (Python Software Foundation) that enabled automatic measurement of 3 types of choroidal metrics: (1) CT, (2) choroidal area, and (3) CVI using a similar method to one mentioned by Wang et al.[65] Choroidal metrics were measured for (1) the choriocapillaris plus Sattler's layer and (2) the Haller's layer within the subfovea, as well as the parafoveal region. We intentionally separated the measurements over the subfoveal region because it has been shown that the choroid is thickest subfoveally and thins out nasally and temporally in healthy eyes.[60,66] The subfoveal region is defined as 500 μm from both sides of the center of the fovea, whereas the parafoveal region is defined as the 2-mm area from both sides of the subfoveal region. The thickness of the choriocapillaris plus Sattler's layer was defined as the shortest vertical distance from the hyperreflective line of Bruch's membrane to the inner border of Haller's layer, which is defined as the innermost point of the large choroidal vessel as mentioned above. The thickness of Haller's layer was defined as the shortest vertical distance from its inner border to the CSI, which is defined as the outermost hyperreflective line in the Niblack-filtered image. Instead of using a single-point measurement as in the previous study, CT was calculated based on the average obtained from measurement points at a 100-μm interval to better estimate the actual CT and to reduce the variability. The choroidal vascularity index was defined as the proportion of the luminal area to the total circumscribed choroidal area.

To assess the reliability of measurements or intraobserver variability, the same grader (V.T.T.C.) graded a set of 33 SS OCT images twice, 3 months apart, to assess the intraclass correlation coefficient. The intraclass correlation coefficient between the first and second gradings was > 0.75 for all Haller's layer measurements, demonstrating that the reliability was good. The reliability of the choroid segmentation method used in the present study was also previously shown to be good in a separate study.[65]

Definition of End Points

Digital retinal fundus photographs centered on the macula, and centered photographs of the optic disc were obtained using a nonmydriatic retinal camera (TRC 50DX; Topcon, Inc) after pupils dilated by 0.5% tropicamide and 0.5% phenylephrine. Diabetic retinopathy severity was graded at each visit according to the modified Airlie House classification scale as applied in the ETDRS.[67] Two masked graders (Z.H.S. and F.Y.T.) determined the DR status and the presence of other ocular conditions (e.g., dese cataract) by retinal photographs throughout the follow-up examinations. The interreliability assessments compared with a senior grader by using a weighed κ static were 0.901 and 0.872, and intrareliability were 0.981 and 0.977, respectively. During grading, the uncertain cases were read further by ophthalmologists for final adjudication.

Progression of DR was defined as a 2-step or more increase in severity level at follow-up when compared with baseline, such as from level 21 to level 37 or more, from level 31 to 43 or more, from level 37 to 47 or more, from level 43 to 53 or more, from 47 to 60 or more, and from level 53 to 60 or more. The modified Airlie House classification scale has been validated for objective quantification of retinopathy severity. Even worsening of just 1 step or more was shown to be associated with a 5- to 6-fold increased risk of PDR development and a 3- to 4-fold risk of clinically significant macular edema developing with a high likelihood of vision loss over a period of 4 years.[68] However, considering the intergrader variability associated with this scale, the current study adopted the worsening of ≥ 2 steps on the scale as the outcome variable for predictive modeling.

Measurement of Other Risk Factors

Age was defined as the age at the time of the baseline examination. The duration of DM was defined as the period between the baseline examination, and the date of diagnosis was first recorded by a physician on the patient's chart or in a hospital record system. Mean arterial blood pressure estimates were calculated as diastolic pressure plus one-third pulse pressure. The level of HbA_{1c} was obtained from the most updated blood tests documented within each patient's medical record.

Sample Size Justification

We estimated that approximately 18% of study participants would demonstrate DR progression over 2 years. A sample size of 101 eyes at baseline would allow us to have > 80% power ($\alpha = 0.05$) to detect a hazard ratio (HR) of 2.1 for DR progression.

Statistical Analysis

All statistical analyses were performed using R software version 3.5.3 (R Foundation for Statistical Computing, Vienna, Austria). Each eye was regarded as the unit of analysis. For all statistical analyses, $P < 0.05$ was considered to be statistically significant.

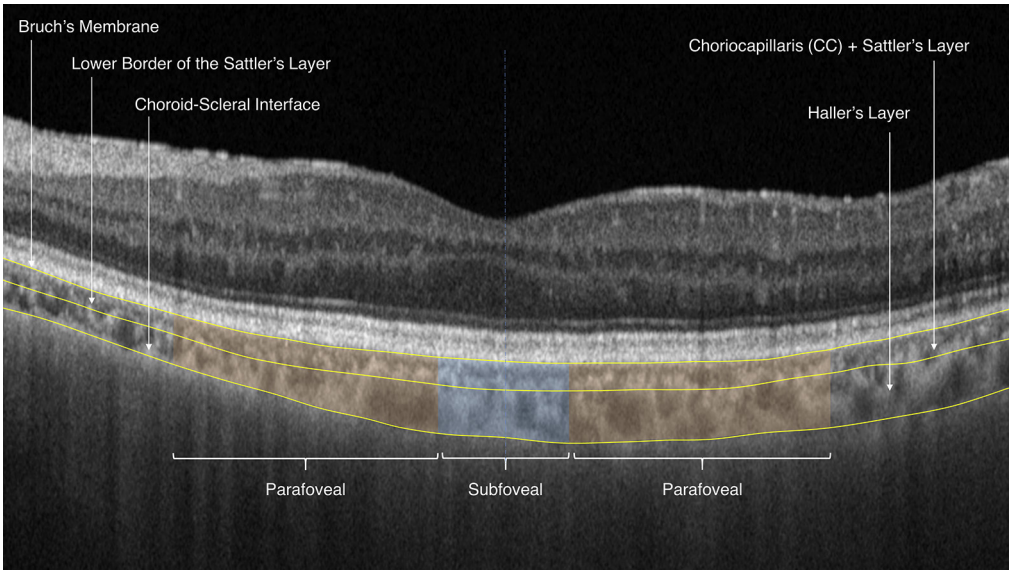

Figure 1. Annotated OCT image showing normal anatomic features of the choroid. The choroid was grossly segmented into 2 layers in this study. The inner choroidal layer includes the region between Bruch's membrane and the lower border of Sattler's layer and corresponds to the choriocapillaris and Sattler's layer (small to medium choroidal vessels). The outer choroidal layer includes the region between the lower border of the Sattler's layer and the choroid-sclera interface, which corresponds to Haller's layer (large choroidal vessels). In the present study, a spectrum of swept-source OCT metrics were measured for each layer within both the subfoveal and parafoveal regions. The subfoveal region (blue shaded region) is defined as 500 μm from both sides of the center of the fovea, whereas the parafoveal region (orange shaded region) is defined as the area 2 mm from both sides of the subfoveal region.

Generalized linear mixed models were used to compare baseline characteristics and choroidal metrics between eyes with different DR severity, adjusted for intereye correlation. Cox proportional hazards models were performed to estimate the relationship of baseline choroidal metrics with the risk of 2-step DR progression. A shared frailty model following γ distribution was used to adjust for correlation between fellow eyes to account for the fact that participants contributed 2 eyes to the study, which are more likely to share similar characteristics to each other than to other patient eyes, violating the assumption that each eye is independent. The first model adjusted only for the confounders of choroidal measurement, including age and axial length.[69–72] The second model additionally adjusted for risk factors of DR progression, including duration of DM, HbA_{1c} levels, body mass index (BMI), MABP, and use of insulin.[73,74] Evaluation of the additional predictive value of choroidal vascular parameters was carried out by computing the C statistic (change in area under the receiver operating characteristic curve) when choroidal metrics were added to the full model based on traditional DR risk factors using the method previously described by DeLong et al.[75]

Results

Participants' Demographic and Clinical Characteristics

A total of 103 eyes from 62 participants were included in the study, including 42 diabetic eyes without DR, 32 eyes with mild NPDR, and 29 eyes with moderate to severe NPDR. Table 1 summarizes the demographic and baseline characteristics of the included participants. No significant difference was found in age, sex, duration of DM, baseline HbA_{1c} level, MABP, BMI, logarithm of the minimum angle of resolution VA, axial length, or intraocular pressure across all groups. Over a mean follow-up period of 34.3 months, 19 eyes (18.4 %) demonstrated a 2-step progression of DR.

Associations of Baseline Choroidal Metrics with Diabetic Retinopathy Severity

Table S2 and Figure S1 present the associations of baseline choroidal metrics with DR severity. In both univariate and multivariate analyses adjusting for within-participant intereye correlation, none of the choroidal metrics were associated with the severity of DR.

Cox Regression Models

Table 2 and Figure 3 show the relationships between baseline choroidal metrics and the risk of 2-step DR progression. After adjusting for age, axial length, and intereye correlation, several choroidal metrics in Haller's layer were associated with a higher risk of DR progression, including subfoveal choroidal area (HR, 2.033; 95% confidence interval [CI], 1.179−3.505; $P = 0.011$), subfoveal plus parafoveal choroidal area (HR, 1.909; 95% CI, 1.096−3.326; $P = 0.022$), subfoveal CT (HR, 2.032; 95% CI, 1.181−3.498; $P = 0.010$), and subfoveal plus parafoveal CT (HR, 1.908; 95% CI, 1.097−3.319; $P = 0.022$). The statistical significance remained (i.e., $P < 0.05$) after additionally adjusting for duration of DM, HbA_{1c} level, BMI, use of insulin, and MABP.

Similar associations with higher hazard of DR progression were observed for choroidal metrics of the entire choroidal layer after adjusting for age, axial length, and intereye correlation, including subfoveal choroidal area (HR, 1.858; 95% CI, 1.019−3.388; $P = 0.043$), subfoveal plus parafoveal choroidal area (HR, 1.778; 95% CI,

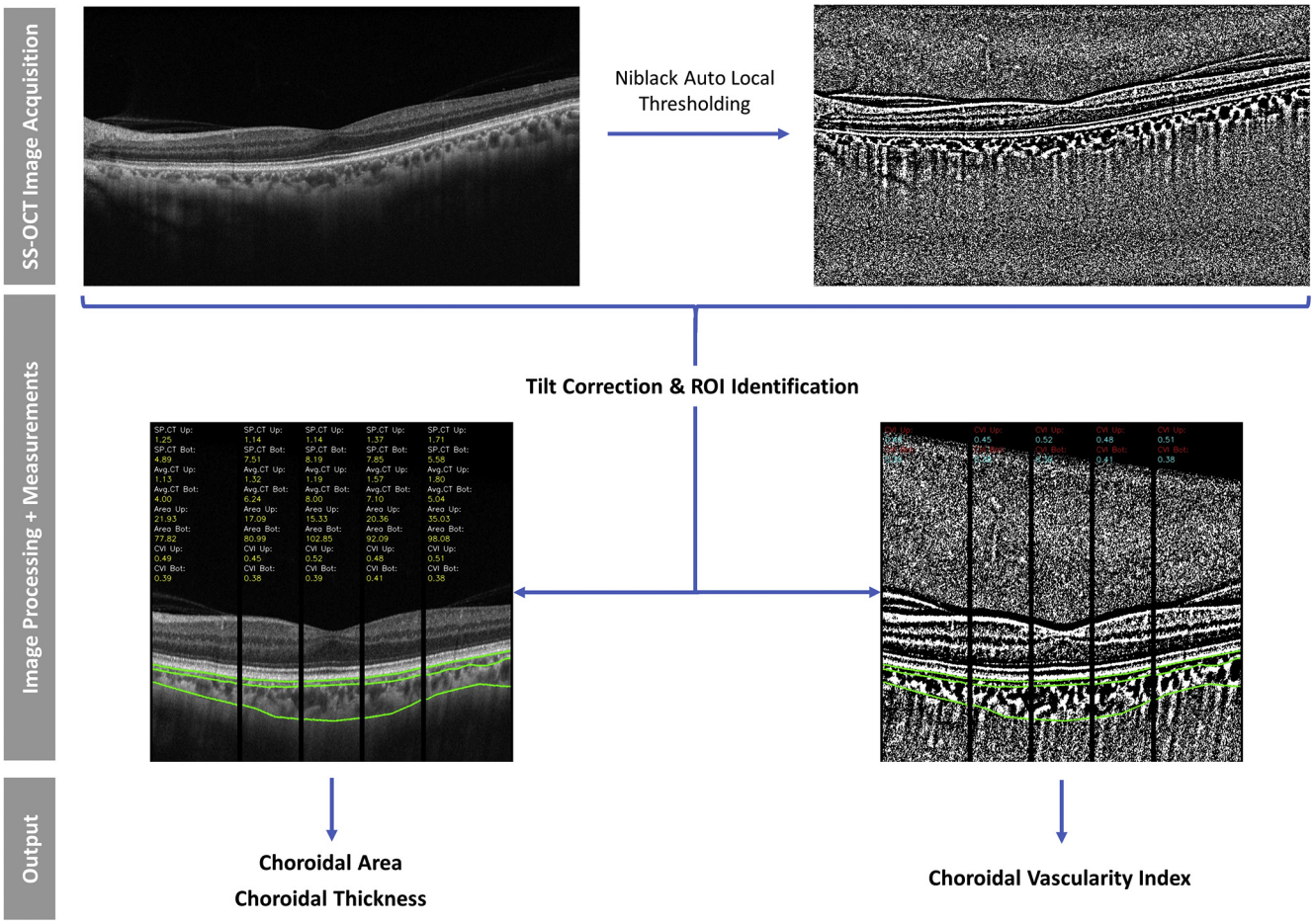

Figure 2. Annotated images showing measurement of choroidal metrics. The choroid was first imaged using swept-source (SS) OCT. A 9-mm SS OCT scan image passing through the fovea horizontally was chosen for each eye. The raw SS OCT image was binarized using Niblack autolocal thresholding. Then, the choriocapillaris—Sattler's layer complex and Haller's layer were identified by manually delineating the Bruch's membrane, the lower border of Sattler's layer, and the choroid-sclera interface. The annotated images were then fed into a customized Python program, which corrected the image tilting and identified the region of interest (ROI; i.e., the subfovea and the subfoveal plus parafoveal region). Finally, 3 choroidal metrics were measured in each ROI, including choroidal area, choroidal thickness, and choroidal vascularity index.

Table 1. Baseline Characteristics of Subjects

Characteristics	Unit	DM without DR (n = 42)	Mild NPDR (n = 32)	Moderate to Severe NPDR (n = 29)	*P* value [1]
Age	Year	65.21 ± 8.52	67.79 ± 7.42	63.48 ± 7.98	0.929
Gender	F/M	28/14	16/16	13/16	0.583
Duration of DM	Year	11.01 ± 7.86	19.32 ± 8.90	13.06 ± 6.82	0.458
Baseline HbA_{1c}	%	6.92 ± 0.80	7.60 ± 1.02	7.35 ± 0.87	0.452
MABP	mmHg	102.80 ± 12.88	96.91 ± 11.00	99.99 ± 13.99	0.901
Body mass index	kg/m^2	25.91 ± 5.12	25.97 ± 4.38	26.30 ± 4.55	0.552
LogMAR	N/A	0.652 ± 0.211	0.703 ± 0.164	0.745 ± 0.211	0.220
Axial length	Mm	23.79 ± 1.46	23.93 ± 1.13	24.00 ± 1.21	0.889
IOP	mmHg	16.80 ± 3.07	15.33 ± 3.01	16.87 ± 2.34	0.714

Demographic and clinical characteristics between different groups were compared using generalized linear mixed model adjusting for within-subject inter-eye correlation.
DM = diabetes mellitus; DR = diabetic retinopathy; F/M = female to male ratio; IOP = intraocular pressure; MABP = mean arterial blood pressure; NPDR = non-proliferative diabetic retinopathy; SD = standard deviation.

Table 2. Cox Regression Models assessing the Relationship of Choroidal Changes with 2-Steps Progression of Diabetic Retinopathy

	Model 1		Model 2	
	HR (95% CI)	P *value*	*HR (95% CI)*	P *value*
Choroidal area (per SD increase)				
CC + Sattler's layer				
Subfoveal	0.705 (0.383 − 1.295)	0.260	−	−
Subfoveal + parafoveal	0.976 (0.563 − 1.691)	0.930	−	−
Haller's layer				
Subfoveal	2.033 (1.179 − 3.505)	**0.011***	2.463 (1.286 − 4.718)	**0.0066***
Subfoveal + parafoveal	1.909 (1.096 − 3.326)	**0.022***	2.455 (1.247 − 4.834)	**0.0093***
All three layers				
Subfoveal	1.858 (1.019 − 3.388)	**0.043***	2.239 (1.080 − 4.642)	**0.030***
Subfoveal + parafoveal	1.778 (0.996 − 3.173)	0.051	2.213 (1.058 − 4.627)	**0.035***
Choroidal thickness (per SD increase)				
CC + Sattler's layer				
Subfoveal	0.700 (0.380 − 1.291)	0.250	−	−
Subfoveal + parafoveal	0.963 (0.555 − 1.673)	0.890	−	−
Haller's layer				
Subfoveal	2.032 (1.181 − 3.498)	**0.010***	2.445 (1.285 − 4.653)	**0.0065***
Subfoveal + parafoveal	1.908 (1.097 − 3.319)	**0.022***	2.448 (1.246 − 4.809)	**0.0094***
All three layers				
Subfoveal	1.867 (1.026 − 3.397)	**0.041***	2.244 (1.089 − 4.626)	**0.028***
Subfoveal + parafoveal	1.779 (0.998 − 3.172)	0.051	2.209 (1.058 − 4.612)	**0.035***
CVI (per SD increase)				
CC + Sattler's layer				
Subfoveal	1.284 (0.785 − 2.101)	0.320	−	−
Subfoveal + parafoveal	1.186 (0.734 − 1.916)	0.490	−	−
Haller's layer				
Subfoveal	1.233 (0.764 − 1.988)	0.390	−	−
Subfoveal + parafoveal	1.507 (0.897 − 2.533)	0.120	−	−

Model 1: Multivariate cox regression models adjusted for age and axial length.
Model 2: Multivariate cox regression models adjusted for baseline severity of diabetic retinopathy, age, axial length, duration of diabetes, glycated haemoglobin level, body mass index, use of insulin, and mean arterial pressure.
In all analyses, inter-eye correlation was resolved using frailty model with gamma distribution.
CC = choriocapillaris; CI = confidence interval; CVI = choroidal vascularity index; HR = hazard ratio.
*P value was < 0.05 and hence statistical significance.

0.996−3.173; $P = 0.051$), subfoveal CT (HR, 1.867; 95% CI, 1.026−3.397; $P = 0.41$), and subfoveal plus parafoveal CT (HR, 1.779; 95% CI, 0.998−3.172; $P = 0.051$). The statistical significance remained (i.e., $P < 0.05$) after additionally adjusting for duration of DM, HbA_{1c} level, use of insulin, BMI, and MABP. The CVI was not significantly associated with DR progression in either model.

We also performed a subgroup analysis to examine whether choroidal metrics were associated with DR progression among eyes without moderate to severe NPDR. Of the 42 diabetic eyes without DR and 32 eyes with mild NPDR at the baseline visit, 16 eyes eventually demonstrated ≥2 steps of progression of DR. Similar to our primary findings, choroidal area and CT of Haller's layer were significantly associated with progression of DR after adjusting for covariates, as shown in Table S3.

Performance Measures of Prediction Models

Table 3 shows the C-statistic for Cox regression models predicting DR progression before and after choroidal metrics were added into the model using established risk factors alone (i.e., duration of DM, HbA_{1c} level, BMI, MABP, use of insulin, and axial length). Based on the findings from Table 2, outer choroidal area and outer CT of subfoveal and subfoveal plus parafoveal regions were added in the calculation of C-statistic for the Cox regression models of DR progression. Models with the inclusion of outer choroidal area and outer CT of subfoveal and subfoveal plus parafoveal regions significantly improved the predictive discrimination for DR progression compared with models using established risk factors alone, with increases in C-statistic ranging from 8.08% to 9.67% ($P < 0.05$).

Discussion

In the current study, we examined a spectrum of choroidal metrics in choroidal sublayers using SS OCT and assessed their associations with the severity of DR and the risk of DR progression, respectively. To summarize, eyes with a larger choroidal area and CT in Haller's layer at baseline were associated with a higher risk of DR progression over 2 years of follow-up. Such associations were independent of age, axial length, and established risk factors, including duration

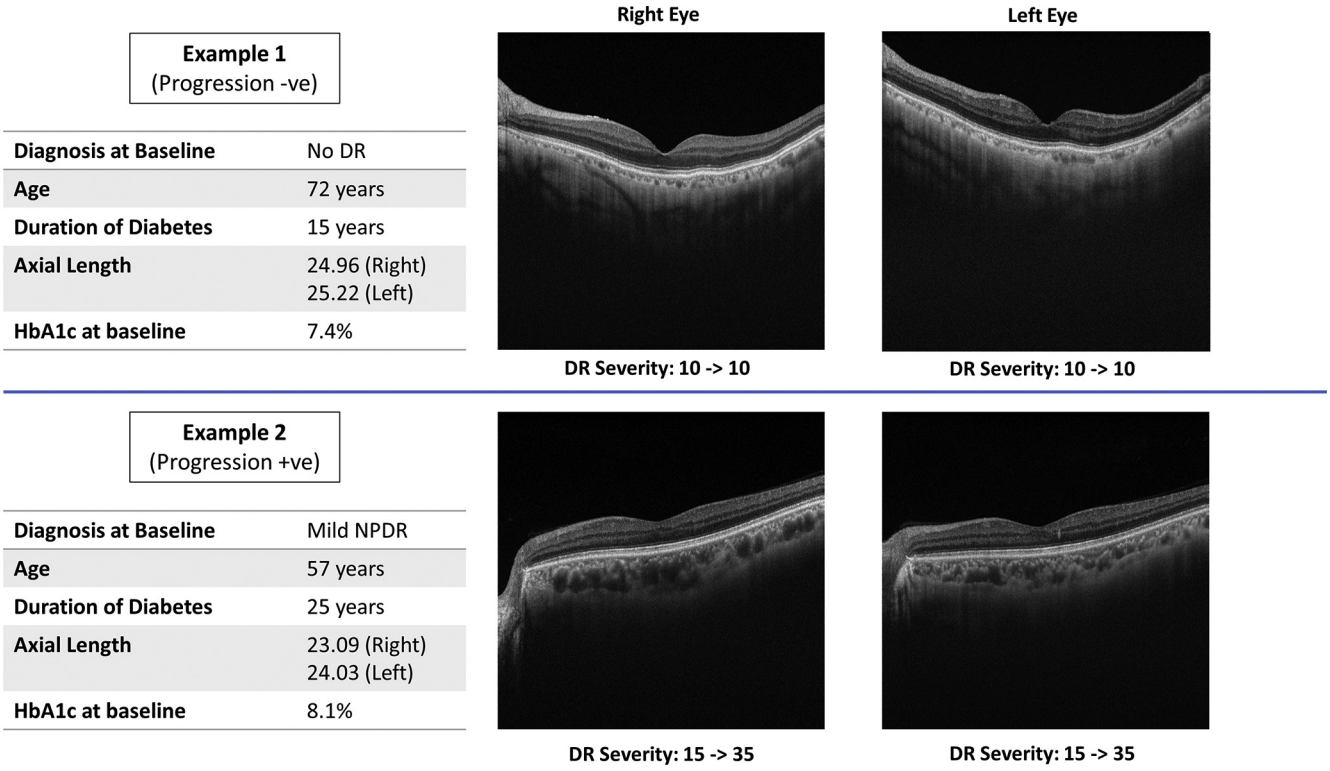

Figure 3. Baseline swept-source OCT images comparing a participant who demonstrated diabetic retinopathy (DR) progression and a participant who did not. This figure illustrates the association of baseline choroidal thickness with the risk of DR progression. The participant (participant 152) with DR progression harbored a significantly thinner choroidal layer after 2 years when compared with the participant who did not show DR progression (participant 146). HbA_{1c} = glycated hemoglobin; NPDR = nonproliferative diabetic retinopathy.

of DM, HbA_{1c} level, BMI, use of insulin, and MABP. The addition of these choroidal metrics significantly improved the discrimination for DR progression when compared with the models using established risk factors alone.

Our findings provide new longitudinal evidence to demonstrate the predictive value of choroidal metrics, which are indicative of diabetic choroidopathy, for progression of DR. Despite the technological advancements in studying retinal structure and function, the underlying pathophysiologic features of DR are not yet fully understood. Choroidopathy has been suggested to play a pivotal role in the pathogenesis of DR[5] in both histopathologic and clinical studies. Histopathologic studies have shown that DR is associated with atrophy and dropout of the choriocapillaris,[7,76,77] leading to functional impairment of the avascular fovea. The dropout of the choriocapillaris could also increase vascular resistance, leading to decreased choroidal blood flow even before the clinical manifestations of DR.[9] Damage to the choroidal layer at the fovea may also cause tissue hypoxia and subsequently increase the level of vascular endothelial growth factor (VEGF), causing neovascularization, and leading to the breakdown of the blood–retina barrier and hence the development of macular edema.[78–80] Subsequent clinical studies with modern imaging techniques have further elucidated the details of diabetic choroidopathy clinically and have reaffirmed the findings from histopathologic studies. For instance, it has been shown that the choroidal vascular abnormalities in diabetic eyes are similar to those of DR, including microaneurysms, dilatation and obstruction of the choriocapillaris, vascular remodeling

Table 3. Predictive Discrimination for DR Progression with and without Choroidal Metrics in the Cox Regression Models Based on Established Risk Factors

Models	C-Statistic	Change in C-Statistic	*P* value (ANOCA)
Established risk factor*	0.755	Reference	–
+ Macular choroidal area of Haller's layer	0.816	0.061 (8.08%)	0.0023*
+ Macular choroidal thickness of Haller's layer	0.818	0.063 (8.34%)	0.0023*
+ Subfoveal choroidal area of Haller's layer	0.828	0.073 (9.67%)	0.0012*
+ Subfoveal choroidal thickness of Haller's layer	0.828	0.073 (9.67%)	0.0016*

*Established risk factors include duration of diabetes, glycated haemoglobin level, body mass index, mean arterial pressure, use of insulin, and axial length.

with increased vascular tortuosity, vascular dropout, areas of vascular nonperfusion, and choroidal neovascularization.[5,7,8,77] Diabetic eyes also showed a significant amount of choriocapillary degeneration[8] and reduction in choroidal blood flow.[81]

In our subgroup analyses, we further illustrated that the association of larger choroidal area and thickness in Haller's layer with the risk of DR progression was statistically significant only among eyes with mild NPDR or no DR, but not among eyes with moderate to severe NPDR. Our findings are in agreement with previous studies that observed total choroidal thickening in the early stage of DR.[20,24,26,38] Consistently, Kim et al[18] also showed an initial phase of choroidal thickening in eyes with mild NPDR before its thinning in more advanced stages of DR. A longitudinal study by Tavares Ferreira et al[24] also observed an increase of CT in diabetic patients without DR after 1 year, while a trend for choroid thinning was observed in diabetic patients with DR when compared with patients without DR.

Interestingly, previous studies found that one of the protective factors against DR is high myopia[82]; eyes with high myopia show thinner CT than healthy control eyes.[83] The mechanism underlying the protective effect of high myopia may be related to the lower level of VEGF.[84,85] Some studies postulated that excessive axial elongation of the eyeballs in high myopia leads to greater intraocular volume and neurodysfunction of the outer retina, both of which result in a reduced concentration of VEGF and hence a lower risk of DR.[86–89] This sheds insights on the potential pathophysiologic features underlying diabetic choroidopathy.

Given that the choroidal area and thickness in Haller's layer could predict the 2-year risk of DR progression, choroidal metrics could be used with traditional DR prognostic factors to identify patients with a higher risk of DR progression. These patients can then receive earlier treatment and closer monitoring to delay or possibly prevent progression to PDR. As funduscopic examination may show no visible retinopathy in patients with a long duration of DM, assessment of outer CT may also serve as a valuable predictive marker for the risk of DR progression. Future research may further explore the temporal relationship between retinal and choroidal microvascular changes in DR and validate whether choroidopathy precedes retinopathy in DM. Studies to assess whether choroidal metrics could predict the development of PDR and DME, and even visual outcome and treatment response, are also warranted.[90]

Although a thicker choroid is associated with a higher risk of DR progression, we did not find any cross-sectional association of the baseline choroidal metrics with the baseline severity of DR. This discrepancy may be the result of a nonlinear relationship between choroidal thickness and severity of DR, in which CT may first increase in the early stage of DR, and then decrease with DR progression.[38] In line with our findings, several studies also found no statistical difference of CT between eyes with different levels of NPDR severity.[16,29] We also did not find any associations of CVI with the DR severity and the risk of DR progression. Choroidal vascularity index has been proposed as an indirect measurement of choroidal vascularity with the aim of overcoming the physiologic variation of CT.[91] However, the estimation of luminal areas may be confounded by the presence of fluid which is also represented as a hyporeflective area,[92] or the caption of tangentially aligned vessels.[61] In addition, CVI is a combined measurement of both luminal area and stromal area of the choroid. As illustrated in a previous study by Tan et al,[63] when the magnitude of increase in luminal area was less than that of total choroidal area, it could manifest mathematically as no change or a reduction in CVI.

The mechanism underlying the association of larger CT and choroidal area with a higher risk of DR progression remains largely unknown. This may be related to VEGF production, which is secreted by retinal pigmented epithelium to the choroidal vasculature in response to ischemia or hypoxia resulting from vascular dropout.[80,93,94] The VEGF then acts on receptors in both the choriocapillaris and large choroidal blood vessels in a paracrine manner.[94,95] In addition to trophic action, VEGF also leads to vasodilatation of middle and large choroidal vessels and increases vascular permeability,[96] leading to increased CT. Consistently, previous studies also attributed decreased choroidal blood flow after laser panretinal photocoagulation to the downregulation of VEGF.[97,98] Furthermore, a thicker choroid is also associated with potential exudative complications, which in turn contribute to the greater rate of progression of DR.[18]

The strengths of our study include the prospective study design, longitudinal follow-up, use of SS OCT, and adjustment of multiple confounding factors that affect the choroid. Swept-source OCT has a longer wavelength, faster scanning speed, and invisible scanning light. This achieves biopsy-like visualization of the choroid, allowing better evaluation of the choroidal sublayers. Our analyses also adjusted for multiple confounding factors that affect CT, including age,[47] axial length,[48] HbA_{1c} level,[22,30,50] use of insulin,and duration of DM.[20] However, we acknowledge several limitations in this study. First, we included only eyes with good-quality images, which may have introduced selection bias and limited the generalizability of results. Second, the follow-up period of this study was relatively short. Third, the small sample size of our study limited the statistical power of our analyses. Future studies are required to further evaluate the role of CVI in predicting DR progression.

In conclusion, the choroidal area and CT of the Haller's layer at baseline are associated with the risk of DR progression, and the addition of these choroidal metrics further improves predictive discrimination of DR progression. Choroidal thickening in the Haller's layer at baseline, or the lack thereof, may help to identify diabetic patients with greater risk of DR progression, who require closer monitoring and more aggressive DM control. Our findings also offer new insights into the role of diabetic choroidopathy in DR progression and support the consideration of choroidal metrics in the routine assessment of DR.

Acknowledgment

The authors would like to thank Dr. Fang Yao Tang for grading the severity of diabetic retinopathy in the present study.

Footnotes and Disclosures

Originally received: September 4, 2021.
Final revision: February 14, 2022.
Accepted: February 18, 2022.
Available online: February 25, 2022. Manuscript no. XOPS-D-21-00161

Department of Ophthalmology and Visual Sciences, The Chinese University of Hong Kong, Hong Kong Special Administrative Region, China.

Disclosure(s):
All authors have completed and submitted the ICMJE disclosures form.
The author(s) have no proprietary or commercial interest in any materials discussed in this article.
Supported by the Chinese University of Hong Kong, Hong Kong Special Administrative Region, China (grant no.: 4054487). The sponsor or funding organization had no role in the design or conduct of this research.

HUMAN SUBJECTS: Human subjects were included in this study. This prospective, observational cohort study adhered to the tenets of the Declaration of Helsinki and was approved by the research ethics committee of Hong Kong Eye Hospital. Written informed consent was obtained from all participants or their respective primary caregivers after a detailed explanation of the study.

No animal subjects were included in this study.

Author Contributions:

Conception and design: Kung, V.T.T. Chan, Wang, Shi, Cheung

Analysis and interpretation: Kung, V.T.T. Chan, Tang, Yang, Sun, Cheung

Data collection: Kung, V.T.T. Chan, C.H. Chan, Kwan, Tang, Shi

Obtained funding: N/A; Study was performed as part of regular employment duties at The Chinese University of Hong kong (CUHK), with support from the direct grant of CUHK.

Overall responsibility: Kung, V.T.T. Chan, Tang, Yang, Sun, Wang, Cheung

Abbreviations and Acronyms:
BMI = body mass index; **CT** = choroidal thickness; **CVI** = choroidal vascularity index; **CI** = confidence interval; **CSI** = choroid−sclera interface; **DR** = diabetic retinopathy; **DM** = diabetes mellitus; **DME** = diabetic macular edema; **HbA_{1c}** = glycated hemoglobin; **HR** = hazard ratio; **MABP** = mean arterial blood pressure; **NPDR** = nonproliferative diabetic retinopathy; **PDR** = proliferative diabetic retinopathy; **SS** = swept-source; **VA** = visual acuity; **VEGF** = vascular endothelial growth factor.

Keywords:
Choroid, Diabetic choroidopathy, Diabetic retinopathy, DR progression, Swept-source OCT.

Correspondence:
Carol Y. Cheung, PhD, Department of Ophthalmology and Visual Sciences, The Chinese University of Hong Kong, 4/F Hong Kong Eye Hospital, 147K Argyle Street, Kowloon, Hong Kong Special Administrative Region, China. E-mail: carolcheung@cuhk.edu.hk.

References

1. Yau JWY, Rogers SL, Kawasaki R, et al. Global prevalence and major risk factors of diabetic retinopathy. *Diabetes Care*. 2012;35(3):556−564.
2. Duh EJ, Sun JK, Stitt AW. Diabetic retinopathy: current understanding, mechanisms, and treatment strategies. *JCI Insight*. 2017;2(14):e93751.
3. Cunha-Vaz J, Faria De Abreu JR, et al. Early breakdown of the blood-retinal barrier in diabetes. *Br J Ophthalmol*. 1975;59(11):649−656.
4. Ciulla TA, Harris A, Latkany P, et al. Ocular perfusion abnormalities in diabetes. *Acta Ophthalmol Scand*. 2002;80(5):468−477.
5. Melancia D, Vicente A, Cunha JP, et al. Diabetic choroidopathy: a review of the current literature. *Graefes Arch Clin Exp Ophthalmol*. 2016;254(8):1453−1461.
6. Campos A, Campos EJ, Martins J, et al. Viewing the choroid: where we stand, challenges and contradictions in diabetic retinopathy and diabetic macular oedema. *Acta Ophthalmol*. 2017;95(5):446−459.
7. Hidayat AA, Fine BS. Diabetic choroidopathy: light and electron microscopic observations of seven cases. *Ophthalmology*. 1985;92(4):512−522.
8. Langham ME, Grebe R, Hopkins S, et al. Choroidal blood flow in diabetic retinopathy. *Experimental Eye Research*. 1991;52(2):167−173.
9. Nagaoka T, Kitaya N, Sugawara R, et al. Alteration of choroidal circulation in the foveal region in patients with type 2 diabetes. *Br J Ophthalmol*. 2004;88(8):1060−1063.
10. Mrejen S, Spaide RF. Optical coherence tomography: Imaging of the choroid and beyond. *Surv Ophthalmol*. 2013;58(5):387−429.
11. Cao J, McLeod DS, Merges CA, Lutty GA. Choriocapillaris degeneration and related pathologic changes in human diabetic eyes. *Arch Ophthalmol*. 1998;116(5):589−597.
12. Fryczkowski AW, Sato SE, Hodes BL. Changes in the diabetic choroidal vasculature: scanning electron microscopy findings. *Ann Ophthalmol*. 1988;20(8):299−305.
13. Lutty GA. Diabetic choroidopathy. *Vision Res*. 2017;139:161−167.
14. Shiragami C, Shiraga F, Matsuo T, et al. Risk factors for diabetic choroidopathy in patients with diabetic retinopathy. *Graefes Arch Clin Exp Ophthalmol*. 2002;240(6):436−442.
15. Kim M, Ha MJ, Choi SY, Park Y-H. Choroidal vascularity index in type-2 diabetes analyzed by swept-source optical coherence tomography. *Sci Rep*. 2018;8:70.
16. Querques G, Lattanzio R, Querques L, et al. Enhanced depth imaging optical coherence tomography in type 2 diabetes. *Invest Ophthalmol Vis Sci*. 2012;53:6017−6024.
17. Esmaeelpour M, Považay B, Hermann B, et al. Mapping choroidal and retinal thickness variation in type 2 diabetes using three-dimensional 1060-nm optical coherence tomography. *Invest Ophthalmol Vis Sci*. 2011;52(8):5311−5316.
18. Kim JT, Lee DH, Joe SG, et al. Changes in choroidal thickness in relation to the severity of retinopathy and macular edema in type 2 diabetic patients. *Invest Ophthalmol Vis Sci*. 2013;54(5):3378−3384.
19. Endo H, Kase S, Saito M, et al. Choroidal thickness in diabetic patients without diabetic retinopathy: a meta-analysis. *Am J Ophthalmol*. 2020;218:68−77.
20. Xu J, Xu L, Du KF, et al. Subfoveal choroidal thickness in diabetes and diabetic retinopathy. *Ophthalmology*. 2013;120(10):2023−2028.
21. Adhi M, Brewer E, Waheed NK, Duker JS. Analysis of morphological features and vascular layers of choroid in diabetic retinopathy using spectral-domain optical coherence tomography. *JAMA Ophthalmol*. 2013;131(10):1267−1274.

22. Ünsal E, Eltutar K, Zirtiloğlu S, et al. Choroidal thickness in patients with diabetic retinopathy. *Clin Ophthalmol*. 2014;8:637–642.
23. Rewbury R, Want A, Varughese R, Chong V. Subfoveal choroidal thickness in patients with diabetic retinopathy and diabetic macular oedema. *Eye*. 2016;30:1568–1572.
24. Tavares Ferreira J, Proença R, Alves M, et al. Retina and choroid of diabetic patients without observed retinal vascular changes: a longitudinal study. *Am J Ophthalmol*. 2017;176:15–25.
25. Wang JC, Laíns I, Providência J, et al. Diabetic choroidopathy: choroidal vascular density and volume in diabetic retinopathy with swept-source optical coherence tomography. *Am J Ophthalmol*. 2017;184:75–83.
26. Tavares Ferreira J, Vicente A, Proença R, et al. Choroidal thickness in diabetic patients without diabetic retinopathy. *Retina*. 2018;38(4):795–804.
27. Ohara Z, Tabuchi H, Nakakura S, et al. Changes in choroidal thickness in patients with diabetic retinopathy. *Int Ophthalmol*. 2018;38(1):279–286.
28. Endo H, Kase S, Takahashi M, et al. Alteration of layer thickness in the choroid of diabetic patients. *Clin Exp Ophthalmol*. 2018;46(8):926–933.
29. Gupta C, Tan R, Mishra C, et al. Choroidal structural analysis in eyes with diabetic retinopathy and diabetic macular edema—a novel OCT based imaging biomarker. *PLoS One*. 2018;13(12):e0207435.
30. Horváth H, Kovács I, Sándor GL, et al. Choroidal thickness changes in non-treated eyes of patients with diabetes: swept-source optical coherence tomography study. *Acta Diabetol*. 2018;55:927–934.
31. Ambiya V, Kumar A, Baranwal VK, et al. Change in subfoveal choroidal thickness in diabetes and in various grades of diabetic retinopathy. *Int J Retin Vitr*. 2018;4:34.
32. Gołębiewska J, Olechowski A, Wysocka-Mincewicz M, et al. Choroidal thickness and ganglion cell complex in pubescent children with type 1 diabetes without diabetic retinopathy analyzed by spectral domain optical coherence tomography. *J Diabetes Res*. 2018;2018:5458015.
33. Laíns I, Talcott KE, Santos AR, et al. Choroidal thickness in diabetic retinopathy assessed with swept-source optical coherence tomography. *Retina*. 2018;38:173–182.
34. Kinoshita T, Imaizumi H, Shimizu M, et al. Systemic and ocular determinants of choroidal structures on optical coherence tomography of eyes with diabetes and diabetic retinopathy. *Sci Rep*. 2019;9(1):16228.
35. Wang H, Tao Y. Choroidal structural changes correlate with severity of diabetic retinopathy in diabetes mellitus. *BMC Ophthalmol*. 2019;19(1):186.
36. Do Jeong K, Park JY, Kim BN, et al. Assessment of choroidal thickness inside and outside of vascular arcade in diabetic retinopathy eyes using spectral-domain optical coherence tomography. *Sci Rep*. 2019;9(1):10780.
37. Foo VHX, Gupta P, Nguyen QD, et al. Decrease in choroidal vascularity index of Haller's layer in diabetic eyes precedes retinopathy. *BMJ Open Diabetes Res Care*. 2020;8(1):e001295.
38. Wang W, Liu S, Qiu Z, et al. Choroidal thickness in diabetes and diabetic retinopathy: a swept source OCT study. *Invest Ophthalmol Vis Sci*. 2020;61(4):29.
39. Kase S, Endo H, Takahashi M, et al. Alteration of choroidal vascular structure in diabetic macular edema. *Graefes Arch Clin Exp Ophthalmol*. 2020;258(5):971–977.
40. Huang X, Zhang P, Zou X, et al. Thinner average choroidal thickness is a risk factor for the onset of diabetic retinopathy. *Ophthalmic Res*. 2020;63(3):259–270.
41. Endo H, Kase S, Takahashi M, et al. Relationship between diabetic macular edema and choroidal layer thickness. *PLoS One*. 2020;15(1):e0226630.
42. McCourt EA, Cadena BC, Barnett CJ, et al. Measurement of subfoveal choroidal thickness using spectral domain optical coherence tomography. *Ophthalmic Surg Lasers Imaging*. 2010;41(Suppl):S28–S33.
43. Esmaeelpour M, Brunner S, Ansari-Shahrezaei S, et al. Choroidal thinning in diabetes type 1 detected by 3-dimensional 1060 nm optical coherence tomography. *Invest Ophthalmol Vis Sci*. 2012;53(11):6803–6809.
44. Regatieri CV, Branchini L, Carmody J, et al. Choroidal thickness in patients with diabetic retinopathy analyzed by spectral-domain optical coherence tomography. *Retina*. 2012;32(3):563–568.
45. Vujosevic S, Martini F, Cavarzeran F, et al. Macular and peripapillary choroidal thickness in diabetic patients. *Retina*. 2012;32(9):1781–1790.
46. Lee HK, Lim JW, Shin MC. Comparison of choroidal thickness in patients with diabetes by spectral-domain optical coherence tomography. *Korean J Ophthalmol*. 2013;27(6):433–439.
47. Ooto S, Hangai M, Yoshimura N. Effects of sex and age on the normal retinal and choroidal structures on optical coherence tomography. *Curr Eye Res*. 2015;40(2):213–225.
48. Tuncer I, Karahan E, Zengin MO, et al. Choroidal thickness in relation to sex, age, refractive error, and axial length in healthy Turkish subjects. *Int Ophthalmol*. 2015;35(3):403–410.
49. Agrawal R, Ding J, Sen P, et al. Exploring choroidal angioarchitecture in health and disease using choroidal vascularity index. *Prog Retin Eye Res*. 2020;77:100829.
50. Torabi H, Isfeedvajani MS, Ramezani M, Daryabari SH. Choroidal thickness and hemoglobin A1c levels in patients with type 2 diabetes mellitus. *J Ophthalmic Vis Res*. 2019;14(3):285–290.
51. Nickla DL, Wallman J. The multifunctional choroid. *Prog Retin Eye Res*. 2010;29(2):144–168.
52. Gupta P, Cheng CY, Cheung CMG, et al. Relationship of ocular and systemic factors to the visibility of choroidal-scleral interface using spectral domain optical coherence tomography. *Acta Ophthalmol*. 2016;94(2):e142–e149.
53. Agrawal R, Gupta P, Tan KA, et al. Choroidal vascularity index as a measure of vascular status of the choroid: Measurements in healthy eyes from a population-based study. *Sci Rep*. 2016;6:21090.
54. Unterhuber A, Povazay B, Hermann B, et al. In vivo retinal optical coherence tomography at 1040 nm—enhanced penetration into the choroid. *Opt Express*. 2005;13:3252.
55. Park HYL, Shin HY, Park CK. Imaging the posterior segment of the eye using swept-source optical coherence tomography in myopic glaucoma eyes: comparison with enhanced-depth imaging. *Am J Ophthalmol*. 2014;157:550–557.
56. Adhi M, Liu JJ, Qavi AH, et al. Enhanced visualization of the choroido-scleral interface using swept-source OCT. *Ophthalmic Surg Lasers Imaging Retina*. 2013;44(6 Suppl):S40–S42.
57. Ferrara D, Mohler KJ, Waheed N, et al. En face enhanced-depth swept-source optical coherence tomography features of chronic central serous chorioretinopathy. *Ophthalmology*. 2014;121(3):719–726.
58. Adhi M, Liu JJ, Qavi AH, et al. Choroidal analysis in healthy eyes using swept-source optical coherence tomography compared to spectral domain optical coherence tomography. *Am J Ophthalmol*. 2014;157(6):1272–1281.e1.
59. Ramrattan RS, Van der Schaft TL, Mooy CM, et al. Morphometric analysis of Bruch's membrane, the

choriocapillaris, and the choroid in aging. *Invest Ophthalmol Vis Sci*. 1994;35(6):2857−2864.
60. Branchini LA, Adhi M, Regatieri CV, et al. Analysis of choroidal morphologic features and vasculature in healthy eyes using spectral-domain optical coherence tomography. *Ophthalmology*. 2013;120(9):1901−1908.
61. Sonoda S, Sakamoto T, Yamashita T, et al. Choroidal structure in normal eyes and after photodynamic therapy determined by binarization of optical coherence tomographic images. *Invest Ophthalmol Vis Sci*. 2014;55(6):3893−3899.
62. Agrawal R, Salman M, Tan KA, et al. Choroidal vascularity index (CVI)—a novel optical coherence tomography parameter for monitoring patients with panuveitis? *PLoS One*. 2016;11(1):e0146344.
63. Tan KA, Laude A, Yip V, et al. Choroidal vascularity index—a novel optical coherence tomography parameter for disease monitoring in diabetes mellitus? *Acta Ophthalmol*. 2016;94(7):e612−e616.
64. Chen H, Wu Z, Chen Y, et al. Short-term changes of choroidal vascular structures after phacoemulsification surgery. *BMC Ophthalmol*. 2018;18(1):81.
65. Wang YM, Hui VWK, Shi J, et al. Characterization of macular choroid in normal-tension glaucoma: a swept-source optical coherence tomography study. *Acta Ophthalmol*. 2021;99(8):e1421−e1429.
66. Manjunath V, Taha M, Fujimoto JG, Duker JS. Choroidal thickness in normal eyes measured using cirrus HD optical coherence tomography. *Am J Ophthalmol*. 2010;150(3):325−329.e1..
67. Early Treatment Diabetic Retinopathy Study Research Group. Grading diabetic retinopathy from stereoscopic color fundus photographs—an extension of the modified Airlie House classification: ETDRS report number 10. *Ophthalmology*. 2020;127(4S):S99−S119.
68. Klein R, Klein BEK, Moss SE. How many steps of progression of diabetic retinopathy are meaningful? The Wisconsin epidemiologic study of diabetic retinopathy. *Arch Ophthalmol*. 2001;119(4):547−553.
69. Wei WB, Xu L, Jonas JB, et al. Subfoveal choroidal thickness: the Beijing Eye Study. *Ophthalmology*. 2013;120(12):2749−2750.
70. Yasuno Y, Miura M, Kawana K, et al. Visualization of subretinal pigment epithelium morphologies of exudative macular diseases by high-penetration optical coherence tomography. *Invest Ophthalmol Vis Sci*. 2009;50(1):405−413.
71. Považay B, Hermann B, Hofer B, et al. Wide-field optical coherence tomography of the choroid in vivo. *Invest Ophthalmol Vis Sci*. 2009;50(4):1856−1863.
72. Fujiwara T, Imamura Y, Margolis R, et al. Enhanced depth imaging optical coherence tomography of the choroid in highly myopic eyes. *Am J Ophthalmol*. 2009;148(3):445−450.
73. Akay F, Gundogan FC, Yolcu U, et al. Choroidal thickness in systemic arterial hypertension. *European J Ophthalmology*. 2016;26(2):152−157.
74. Endo H, Kase S, Ito Y, et al. Relationship between choroidal structure and duration of diabetes. *Graefes Arch Clin Exp Ophthalmol*. 2019;257(6):1133−1140.
75. DeLong ER, DeLong DM, Clarke-Pearson DL. Comparing the areas under two or more correlated receiver operating characteristic curves: a nonparametric approach. *Biometrics*. 1988;44(3):837−845.
76. Lutty GA, Cao J, McLeod DS. Relationship of polymorphonuclear leukocytes to capillary dropout in the human diabetic choroid. *Am J Pathol*. 1997;151(3):707−714.
77. McLeod DS, Lutty GA. High-resolution histologic analysis of the human choroidal vasculature. *Invest Ophthalmol Vis Sci*. 1994;35(11):3799−3811.
78. Cunha-Vaz JG, Goldberg MF, Vygantas C, Noth J. Early detection of retinal involvement in diabetes by vitreous fluorophotometry. *Ophthalmology*. 1979;86(2):264−275.
79. Mori F, Hikichi T, Takahashi J, et al. Dysfunction of active transport of blood-retinal barrier in patients with clinically significant macular edema in type 2 diabetes. *Diabetes Care*. 2002;25(7):1248−1249.
80. Aiello LP, Northrup JM, Keyt BA, et al. Hypoxic regulation of vascular endothelial growth factor in retinal cells. *Arch Ophthalmol*. 1995;113(12):1538−1544.
81. Kawarai M, Koss MC. Sympathetic vasoconstriction in the rat anterior choroid is mediated by α1-adrenoceptors. *Eur J Pharmacol*. 1998;363(1):35−40.
82. Wang X, Tang L, Gao L, et al. Myopia and diabetic retinopathy: a systematic review and meta-analysis. *Diabetes Res Clin Pract*. 2016;111:1−9.
83. Wang S, Wang Y, Gao X, et al. Choroidal thickness and high myopia: a cross-sectional study and meta-analysis Retina. *BMC Ophthalmol*. 2015;15:70.
84. Chen W, Song H, Xie S, et al. Correlation of macular choroidal thickness with concentrations of aqueous vascular endothelial growth factor in high myopia. *Curr Eye Res*. 2015;40(3):307−313.
85. Ahn SJ, Park KH, Woo SJ. Subfoveal choroidal thickness changes following antivascular endothelial growth factor therapy in myopic choroidal neovascularization. *Invest Ophthalmol Vis Sci*. 2015;56(10):5794−5800.
86. Sawada O, Miyake T, Kakinoki M, et al. Negative correlation between aqueous vascular endothelial growth factor levels and axial length. *Jpn J Ophthalmol*. 2011;55(4):401−404.
87. Man REK, Gan ATL, Gupta P, et al. Is myopia associated with the incidence and progression of diabetic retinopathy? *Am J Ophthalmol*. 2019;208:226−233.
88. Man REK, Lamoureux EL, Taouk Y, et al. Axial length, retinal function, and oxygen consumption: A potential mechanism for a lower risk of diabetic retinopathy in longer eyes. *Invest Ophthalmol Vis Sci*. 2013;54(12):7691−7698.
89. Shin YJ, Nam WH, Park SE, et al. Aqueous humor concentrations of vascular endothelial growth factor and pigment epithelium-derived factor in high myopic patients. *Mol Vis*. 2012;18:2265−2270.
90. Hui VWK, Szeto SKH, Tang F, et al. Optical coherence tomography classification systems for diabetic macular edema and their associations with visual outcome and treatment responses—an updated review. *Asia Pac J Ophthalmol (Phila)*. 2021 Dec 17. https://doi.org/10.1097/APO.0000000000000468.
91. Iovino C, Pellegrini M, Bernabei F, et al. Choroidal vascularity index: an in-depth analysis of this novel optical coherence tomography parameter. *J Clin Med*. 2020;9(2):595.
92. Spaide RF, Ryan EH. Loculation of fluid in the posterior choroid in eyes with central serous chorioretinopathy. *Am J Ophthalmol*. 2015;160(6):1211−1216.
93. Gupta N, Mansoor S, Sharma A, et al. Diabetic retinopathy and VEGF. *Open Ophthalmol J*. 2013;7:4−10.
94. Blaauwgeers HGT, Holtkamp GM, Rutten H, et al. Polarized vascular endothelial growth factor secretion by human retinal pigment epithelium and localization of vascular endothelial growth factor receptors on the inner choriocapillaris: evidence

for a trophic paracrine relation. *Am J Pathol*. 1999;155(2):421–428.

95. Saint-Geniez M, Maldonado AE, D'Amore PA. VEGF expression and receptor activation in the choroid during development and in the adult. *Invest Ophthalmol Vis Sci*. 2006;47(7):3135–3142.
96. Tilton RG, Chang KC, Lejeune WS, et al. Role for nitric oxide in the hyperpermeability and hemodynamic changes induced by intravenous VEGF. *Invest Ophthalmol Vis Sci*. 1999;40(3):689–696.
97. Palanker D, Blumenkranz MS. Panretinal photocoagulation for proliferative diabetic retinopathy. *Am J Ophthalmol*. 2012;153(4):780–781.
98. Geyer O, Neudorfer M, Snir T, et al. Pulsatile ocular blood flow in diabetic retinopathy. *Acta Ophthalmol Scand*. 1999;77(5):522–525.